ORIGINAL ARTICLE

*Journal of Cachexia, Sarcopenia and Muscle* 2022; **13**: 1087–1099
Published online 16 February 2022 in Wiley Online Library (wileyonlinelibrary.com) **DOI:** 10.1002/jcsm.12957

# Altered features of body composition in older adults with type 2 diabetes and prediabetes compared with matched controls

Kirsten E. Bell, Michael T. Paris, Egor Avrutin & Marina Mourtzakis*

*Department of Kinesiology and Health Sciences, University of Waterloo, Waterloo, ON, Canada*

## Abstract

**Background** Ageing is accompanied by muscle loss and fat gain, which may elevate the risk of type 2 diabetes (T2D). However, there is a paucity of data on the distribution of regional lean and fat tissue in older adults with T2D or prediabetes compared with healthy controls. The objective of this study was to compare regional body composition [by dual-energy x-ray absorptiometry (DXA)], muscle and subcutaneous adipose tissue (SAT) thicknesses (by ultrasound), and ultrasound-based muscle texture features in older adults with T2D or prediabetes compared with normoglycaemic controls.

**Methods** Eighteen adults > 60 years with T2D or prediabetes (T2D group) were individually matched to normoglycaemic participants [healthy matched (HM) group] for age (±5 years), sex, and body fat (±2.5%). In a single study visit, all participants received a whole-body DXA scan and ultrasound assessment of the abdomen and anterior thigh. At these two landmarks, we used ultrasound to measure muscle and SAT thickness, as well as texture features of the rectus femoris and rectus abdominis. We also conducted an exploratory subanalysis on a subset of participants ($n$ = 14/18 in the T2D group and $n$ = 10/18 in the HM group) who underwent additional assessments including strength testing of the knee extensors (using a Biodex dynamometer), and a fasting blood sample for the measurement of circulating markers of glucose metabolism [glucose, insulin, c-peptide, and the homoeostatic model assessment of insulin resistance (HOMA-IR)].

**Results** The T2D group was 72 ± 8 years old (mean ± SD), predominantly male ($n$ = 15/18; 83%), and overweight (BMI: 27.8 ± 4.2 kg/m$^2$, 33.2 ± 5.3% body fat). DXA-derived upper arm lean mass was 0.4 kg greater ($P$ = 0.034), and leg fat mass was 1.4 kg lower ($P$ = 0.048), in the T2D vs. HM group. Ultrasound-based texture features were distinct between the groups [rectus abdominis blob size: 0.07 ± 0.06 vs. 0.30 ± 0.43 cm$^2$, $P$ = 0.045; rectus femoris local binary pattern (LBP) entropy: 4.65 ± 0.05 vs. 4.59 ± 0.08 A.U., $P$ = 0.007]. When all participants who underwent additional assessments were pooled ($n$ = 24), we observed that certain ultrasound-based muscle texture features correlated significantly with muscle strength (rectus abdominis histogram skew vs. power during an isokinetic contraction at 60°/s: $r$ = 0.601, $P$ = 0.003) and insulin resistance (rectus femoris LBP entropy vs. HOMA-IR: $r$ = 0.419, $P$ = 0.042).

**Conclusions** Our findings suggest a novel body composition phenotype specific to older adults with T2D or prediabetes. We are also the first to report that ultrasound-based texture features correspond with functional outcomes. Future larger scale studies are needed to uncover the mechanisms underpinning these regional body composition differences.

**Keywords** Muscle; Subcutaneous adipose tissue; Ultrasound; Texture analysis

*Received: 13 July 2021; Revised: 8 December 2021; Accepted: 1 February 2022*
**Correspondence to: Marina Mourtzakis, Department of Kinesiology and Health Sciences – BMH 3033, University of Waterloo, 200 University Avenue West, Waterloo, ON N2L 3G1, Canada. Email: mmourtzakis@uwaterloo.ca*

## Introduction

Ageing is accompanied by muscle atrophy and/or increased adiposity that elevates the risk of type 2 diabetes. Given that skeletal muscle is the primary organ responsible for glucose disposal,[1] low skeletal muscle mass may predispose older individuals to the development of type 2 diabetes. In addition to reduced skeletal muscle mass, fat mass tends to increase with age.[2] Of particular concern is the age-related redistribution of adipose tissue from subcutaneous to visceral and ectopic depots (such as the liver and skeletal muscle),[3] which increases the risk of type 2 diabetes regardless of whole-body fat mass.[4]

Considering the deleterious changes to body composition and metabolism that develop in older age, muscle, and adipose tissue characteristics may be distinct in type 2 diabetics who are older (≥60 years) compared with younger (<40 years) or middle-aged (~40–60 years). Yet many of the existing studies on body composition in this patient population include any adult > 30 years with type 2 diabetes. Of the relatively few studies performed exclusively in older adults with type 2 diabetes, some,[5–9] but not all,[10–12] have observed higher fat mass and/or lower lean mass in patients compared with age-matched normoglycaemic controls. However, percent body fat directly influences the distribution of lean mass in both healthy[13] and diabetic[14] adults. As such, there may be important underlying regional body composition differences (e.g. arms, legs, and trunk) between diabetic and non-diabetic older adults that have yet to be identified. In particular, lean mass may be greater in the weight-bearing lower limbs of heavier individuals as a result of regular ambulation with greater body mass.[15] To date, however, no study has matched diabetic and non-diabetic older adults for % body fat to probe for differences in regional body composition.

Ultrasound is emerging as a versatile tool for site-specific muscle and fat thickness measurements in healthy and clinical populations. Ultrasound is more accessible, safe, and cost-effective than reference body composition technologies such as magnetic resonance imaging, computed tomography, and dual-energy X-ray absorptiometry (DXA). Ultrasound can be used to directly measure not only muscle size (thickness and cross-sectional area), but also tissue composition or texture, which may provide valuable information about non-muscle (i.e. fat and/or fibrotic) tissue infiltration. Muscle echointensity (average pixel brightness) is a first-order texture feature that correlates positively with muscle fat accumulation.[16] Given that intramuscular[17] and intermuscular[18] fat accumulation are positively correlated with insulin resistance, and negatively related to muscle strength,[19] ultrasound texture analysis may be particularly important for understanding muscle health in type 2 diabetes. However, echointensity is a relatively simple measure that may be influenced by limb size, thickness of the overlying subcutaneous adipose tissue (SAT) layer, and instrument settings.[20] Higher order ultrasound texture features (e.g. grey-level co-occurrence matrices, local binary patterns, and blob analysis) are less vulnerable to these variables than echointensity and may provide more in-depth information on muscle tissue quality. Understanding these texture features in older adults with type 2 diabetes is important because ultrasound may offer a novel non-invasive approach towards evaluating metabolic health and muscle strength.

The primary objective of this study was to compare the regional distribution of lean soft tissue and fat mass by DXA, and site-specific muscle and SAT thicknesses by ultrasound in older adults with type 2 diabetes or prediabetes vs. normoglycaemic controls, who were individually matched for age, sex, and % body fat. Our secondary objective was to compare ultrasound-based muscle texture features between these groups. A tertiary objective was to examine the association between ultrasound texture features and functional outcomes, such as glucose metabolism and muscle strength. We hypothesized that lean soft tissue mass and muscle thicknesses would be lower and that fat mass and SAT thicknesses would be greater, in the older adults with type 2 diabetes and prediabetes compared with the matched controls. We further hypothesized that older adults with type 2 diabetes or prediabetes would exhibit significant differences in muscle texture features indicative of poorer muscle quality (e.g. higher echointensity and larger mean blob size) compared with matched controls. Lastly, we hypothesized that higher order ultrasound texture features would correlate significantly with aspects of glucose metabolism and muscle strength.

## Methods

### *Study design*

Two groups of participants were recruited from the Kitchener-Waterloo community for this case–control study: (i) adults > 60 years with type 2 diabetes or prediabetes [collectively referred to as the type 2 diabetes (T2D) group] and (ii) normoglycaemic controls who were individually matched to each diabetic or prediabetic participant for age, sex, and % body fat [the healthy matched (HM) group]. All participants reported to the laboratory after an overnight fast for a single study visit that included a whole-body DXA scan, followed by an ultrasound assessment of the abdomen and anterior thigh. A subset of participants (T2D group: $n$ = 14, HM group: $n$ = 10) underwent a total of three study visits: DXA and ultrasound, as above (Day 1), a blood sample for the measurement of fasting serum glucose, insulin, and c-peptide (Day 2), and physical function and strength

assessments (Days 2–3). Blood samples were always obtained in the morning of Day 2 (prior to physical function and strength assessments) to avoid the confounding effects of acute exercise on circulating metabolic markers.

## *Participants*

Individuals were included in the T2D group if they were (i) ≥60 years and (ii) had a physician diagnosis of type 2 diabetes or prediabetes, or fasting blood glucose > 5.6 mM or 2-h blood glucose > 7.8 mM during a 75-g oral glucose tolerance test. Every participant with type 2 diabetes or prediabetes was individually matched to a non-diabetic control participant for age (±5 years), sex (male or female), and % body fat (±2.5% by DXA) (HM group). Exclusion criteria for all participants were as follows: (i) barium swallow in the previous 3 weeks (due to interference with DXA measurements); (ii) infectious disease; (iii) any form of muscular dystrophy; (iv) stroke resulting in muscular disability; (v) cancer or other metabolic disorder; and (vi) cardiac or gastrointestinal problems.

## *Dual-energy x-ray absorptiometry*

### Positioning

Whole-body and regional lean soft tissue and fat mass were measured using DXA (Hologic Discovery QDR 4500; Hologic, Toronto ON) according to our previously published protocol.[21] A second scan was required for one participant (in the T2D group) who did not fit within the lateral limits of the scanning table. This scan was analysed by summing the left limbs, trunk, and head of one scan, and the right limbs of the second scan, as previously described.[22]

### Regional analysis

Using Hologic software (Version 13.2), whole-body scans were segmented into the head, trunk, left and right arms, and left and right legs by a single investigator according to a standardized protocol. Appendicular lean mass index (in kg/m$^2$) was calculated by summing the lean soft tissue mass of all four limbs and dividing by height squared.[23] Each limb was further segmented into upper and lower portions by bisecting across the medial epicondyle of the humerus (*Figure* 1A) and the tibial plateau.

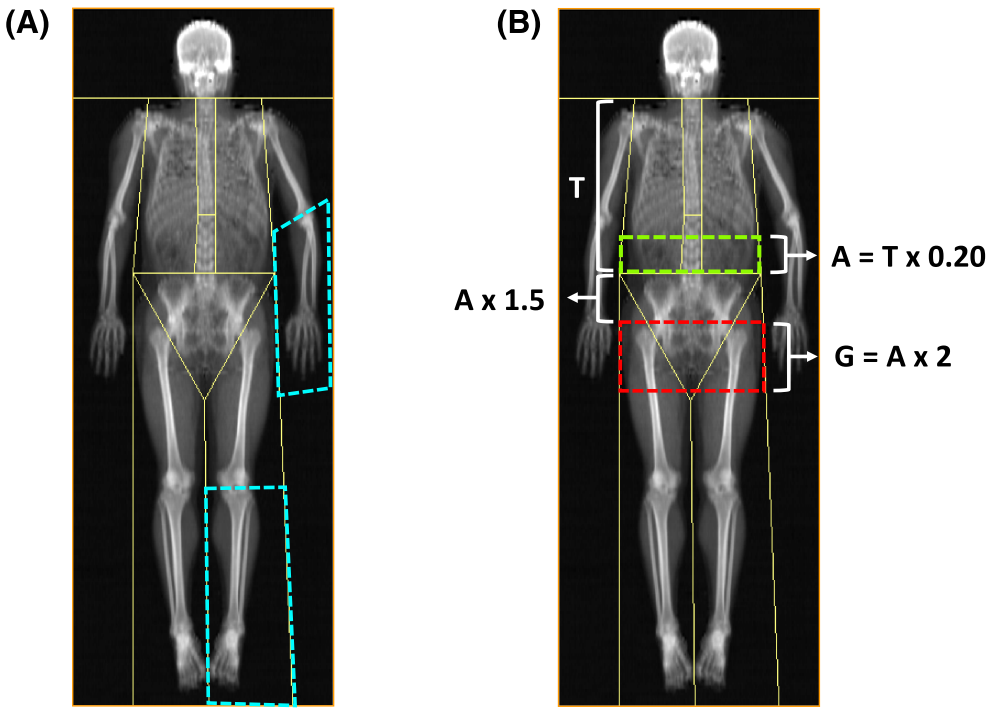


**Figure 1** Landmarks for DXA regional analysis. Thin yellow lines indicate the boundaries between the head, trunk (which included the spine and pelvis), left and right arms, and left and right legs. (*A*) The forearms and lower legs (see dashed blue boxes) were isolated by bisecting across the medial epicondyle of the humerus and tibial plateau. This analysis was performed bilaterally, but for clarity, only the left forearm and left lower leg are highlighted in the figure. (*B*) The android region is indicated by the dashed green box, and the gynoid region is indicated by the dashed red box. The white letter 'T' represents the distance between the horizontal pelvic line and the neck cut line. The height of the android region ('A') was calculated as 20% of the length of 'T'. The horizontal pelvic line was the lower boundary of the android region. The height of the gynoid region was twice the height of the android region. The upper boundary of the gynoid region began below the horizontal pelvic line at a distance equal to 1.5 times 'A'. The lateral limits of the android and gynoid regions were the arm and leg cut lines.

We measured android and gynoid fat mass using the automated analysis included in the Hologic software package. The lower boundary of the android region began at the top of the iliac crests (horizontal pelvic line), and the upper boundary was located 20% of the distance between the horizontal pelvic line and the neck cut line (*Figure* 1B). The height of the gynoid region was twice the height of the android region. The upper boundary of the gynoid region began below the horizontal pelvic line at a distance equal to 1.5 times the height of the android region. The leg cut lines were the lateral limits of the gynoid region. The A/G ratio was calculated by dividing android fat mass by gynoid fat mass.

## *Ultrasound*

## *Landmarking*

Prior to image acquisition, the sites were landmarked using a flexible tape measure and pen while the participants lay supine with their feet hip width apart and secured in place using foot-strap. The foot-strap remained in place during landmarking and image acquisition to prevent excessive internal or external hip rotation, which may influence thigh tissue thickness. Anterior thigh images were taken two-thirds of the distance from the anterior superior iliac spine to the upper pole of the patella. Abdominal images were taken 3 cm to the right of the umbilicus. All ultrasound images were acquired on the right side of the body while participants remained supine.

### Image acquisition

Transverse images of the abdomen and anterior thigh were obtained using a real-time B-mode ultrasound imaging device (M-Turbo, Sonosite) equipped with a multi-frequency linear array transducer (L38xi: 5–10 MHz). Details concerning our instrument settings and probe placement have been previously published.[20]

### Thickness measurements

Abdominal and anterior thigh muscle and SAT thicknesses were measured using ImageJ (Version 1.52a, NIH; Bethesda, MD). Anterior thigh muscle thickness (rectus femoris and vastus intermedius; *Figure* 2A) was obtained by measuring the perpendicular distance between the upper margin of the femur and the rectus femoris fascia, as previously described.[21] Abdominal muscle thickness was obtained by measuring the perpendicular distance between the lower and upper rectus abdominis fascia (*Figure* 2B). SAT thicknesses were obtained by measuring the perpendicular distance between the rectus femoris or rectus abdominis fascia and the skin. Three SAT measurements were taken for each image (*Figure* 2), and the average of these measurements was used in the analysis. A single trained analyst performed all thickness measures.

### Tissue quality

We evaluated tissue quality using ultrasound texture analysis within a specific region of interest (ROI) of the rectus abdominis and rectus femoris muscles. Previously, we showed that ultrasound images of muscle tissue captured on our instrument at a depth of 9.0 cm have distinct texture features compared with images captured at shallower depths (e.g. 7.3, 5.9, and 4.7 cm).[20] As such, in cases where a depth of 9.0 cm was required to optimize the field of view for muscle and SAT thickness measurements, we obtained a second image at 7.3 cm that was used exclusively for texture analysis. For muscle texture analysis, ROIs were manually selected in ImageJ to capture as much of the muscle cross-sectional area as possible while excluding the surrounding muscle fascia (*Figure* 2C,D). To ensure consistent tissue resolution between scans of different depths, each ROI was scaled to a resolution of 0.0153 cm/pixel (corresponding to a depth of 5.9 cm using our equipment) using bilinear interpolation.

Within these ROIs, we assessed several different first-order, second-order, and higher order texture features. First-order features account for individual pixel intensity, independent of spatial distribution, and were extracted from the ROI pixel intensity histogram. The specific first-order features we examined were mean echointensity, skew, kurtosis, energy, and entropy. The mean echointensity of muscle can range from 0 (black) to 255 (white). Histogram kurtosis represents the peakedness of the pixel intensity distribution, with values $> 3$ indicating a leptokurtic (i.e. sharper) peak and values $< 3$ indicating a platykurtic (i.e. flatter) peak. Pixel intensity distribution is normal (i.e. ordinary) when kurtosis is equal to 3.

Second-order and higher order features account for pixel intensity as well as the spatial relationships between pairs of pixels (second-order) or three or more pixels (higher order). Second-order features were extracted from the grey-level co-occurrence matrix (GLCM), which encodes the frequency of pixel pair occurrences at given intensities for a set distance and angle between two pixels.[24] The specific second-order texture features we examined were GLCM energy, contrast, correlation, and homogeneity. These features were averaged across a distance of 5 pixels at angles of 0°, 45°, 90°, and 135° (symmetric matrix).[25] Higher order features were examined using local binary patterns (LBP)[26] and blob analysis.[27] LBP evaluates the local spatial patterns of edges, points, and spots of an image. The specific LBP features we examined were energy and entropy, which were extracted from an LBP image derived using a circular radius of 5 and 8 sampling points.

Blob analysis evaluates the average size of connected islands of white pixels (termed blobs) from a thresholded ultrasound image.[27] Intensity thresholds for the abdomen and anterior thigh landmarks were selected as the 99th percentile

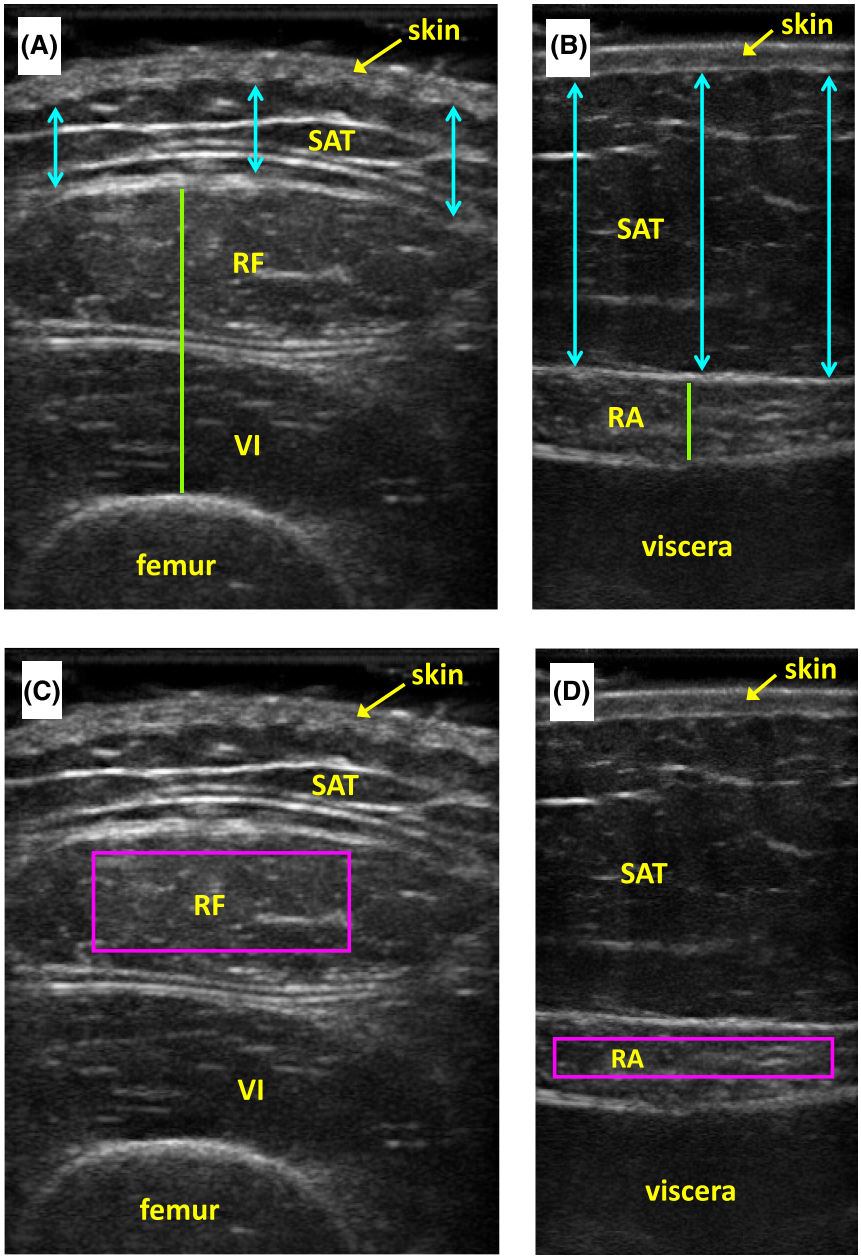


**Figure 2** Placement of ImageJ measurement tools for ultrasound thickness (*A*, *B*) and muscle quality (*C*, *D*) analysis. Green lines indicate where anterior thigh and abdominal muscle thickness measurements were made; blue arrows indicate where anterior thigh and abdominal SAT thickness measurements were made. Purple boxes indicate the ROI where anterior thigh (rectus femoris) and abdominal (rectus abdominis) muscle quality was evaluated. RA, rectus abdominis; RF, rectus femoris; ROI, region of interest; SAT, subcutaneous adipose tissue; VI, vastus intermedius.

from the pixel intensity histogram from a healthy young reference group (rectus femoris—55; rectus abdominis—51, based on unpublished results using our equipment).

### *Physical function and strength assessments*

A subset of participants ($n$ = 14 in the T2D group and $n$ = 10 in the HM group) underwent physical function, strength, and metabolic assessments over two additional study visits. On Day 2, participants received a fasting blood draw followed by five physical function assessments: (i) Short Physical Performance Battery (SPPB), (ii) gait speed, (iii) 6-min walk test (6MWT), (iv) 30-s chair stand test, and (v) grip strength. The SPPB is a standardized test that assesses three key features of physical performance (leg strength, balance, and gait speed) and is scored out of 12 points. The 6MWT was performed on a 20-m course along an indoor hallway.

Participants were instructed to attempt to cover as much distance as possible within 6 min while walking in a safe manner at their usual walking speed. The 30-s chair stand required participants to rise from a chair without the use of their arms as many times as possible in 30 s. We measured grip strength of the left and right hands using a Model J00105 JAMAR® Hydraulic Hand Dynamometer (Performance Health; Warrenville, IL). Participants were seated in a chair with their forearms fixed at 90° flexion and supported by armrests. We verbally encouraged participants to squeeze the dynamometer as hard as possible for 5 s. Participants were given three trials per hand, with 30 s rest in between each trial. The peak strength in kilogrammes for each hand was included in statistical analyses. The SPPB, 6MWT, and 30-s chair stand were each measured once.

We measured isometric and isokinetic strength of the right knee extensors using a Biodex dynamometer (Biodex Medical Systems; Shirley, NY). To increase the accuracy and consistency of our measurements, participants underwent a familiarization session with the Biodex after the physical function assessments on Day 2. One week later, on Day 3, we repeated these measurements. Both Biodex testing days began with a 5-min warm-up at a low-intensity (~25 W) on a stationary bicycle. Participants were then positioned in the dynamometer chair, and chest, waist, mid-thigh, and lower leg straps (secured 5 cm above the inferior aspect of the calcaneus) were used to stabilize the participant and limit extraneous movement. With the knee fixed at 60° flexion, participants were verbally encouraged to perform a 5-s maximal isometric voluntary contraction. Participants performed 3 maximal isometric voluntaries separated by 30 s rest, and the peak torque of each contraction was recorded. Next, we tested isokinetic strength at 60°/s and 180°/s. For each velocity, participants performed three contractions separated by 30 s rest, and the peak torque and maximal power of each contraction was recorded. The average of three trials was analysed.

### *Blood sampling and biochemical analysis*

After an 8–12 h of overnight fast, blood was drawn from an antecubital vein into evacuated collection tubes. The blood was allowed to clot at room temperature for 20 min before centrifugation. The serum was aliquoted and frozen at −80°C for batch analysis.

Glucose was measured spectrophotometrically using the glucose oxidase method, and insulin and c-peptide were measured using commercially available radioimmunoassay kits (Millipore Sigma; Oakville, ON). HOMA-IR was calculated using the following equation:

$$\mathrm{HOMA-IR} = \frac{\text{Fasting glucose}\left(\text{in}\,\frac{\text{mmol}}{\text{L}}\right) \times \text{Fasting insulin}\left(\text{in}\,\frac{\mu\text{IU}}{\text{mL}}\right)}{22.5}$$

### *Statistical analysis*

We used two-tailed paired *t*-tests (T2D vs. HM) to evaluate differences in DXA measures of whole-body and regional lean soft tissue and fat mass, ultrasound measures of muscle and SAT thickness (for the anterior thigh and abdomen), and ultrasound texture features (for the rectus femoris and rectus abdominis).

To better understand the ability of ultrasound to capture aspects of muscle function and glucose metabolism, we conducted an exploratory subanalysis in participants who volunteered to undergo additional testing (T2D group: $n$ = 14, HM group: $n$ = 10). We used independent samples *t*-tests to compare physical function and strength measurements, and circulating metabolic markers, between these two subgroups. In the pooled group of participants ($n$ = 24), we conducted two-tailed Pearson correlations between ultrasound-based muscle measurements (abdominal and anterior thigh muscle and SAT thicknesses, and texture features of the rectus abdominis and rectus femoris) and (ii) physical function and strength outcomes and (ii) circulating markers of glucose metabolism.

Statistical analysis was completed using SPSS (v26.0, IBM Corporation). Statistical significance was accepted as $P < 0.05$. Data are presented as means ± standard deviations, unless otherwise indicated.

## Results

### *Participants*

Participants in the T2D group were 72 ± 8 years old, predominantly male ($n$ = 15 or 83%), and had 33.2 ± 5.3% body fat (*Table* 1). According to BMI, both the T2D and HM groups were overweight on average. There were no between-group differences in these outcomes.

Individuals in the T2D group had been living with either type 2 diabetes ($n$ = 13) or prediabetes ($n$ = 5) for 10 ± 8 years (*Table* 1). Participants managed their diabetes or prediabetes using oral hypoglycaemic medication ($n$ = 11) and/or insulin therapy ($n$ = 3); six participants did not take any anti-diabetic medication. Three participants in the T2D group reported diabetes-related complications (retinopathy, $n$ = 2; nephropathy, $n$ = 1).

The prevalence of additional (i.e., non-diabetic) health conditions was $n$ = 18 in the T2D group and $n$ = 11 in the HM group.

### *Regional lean and fat mass*

Upper arm lean mass was 14% (0.4 kg) greater in the T2D group compared with the HM group ($P$ = 0.034, *Table* 2), while

**Table 1** Physical and clinical characteristics

| | T2D group ($n$ = 18) | HM group ($n$ = 18) | $P$ value |
|---|---|---|---|
| Physical characteristics | | | |
| Age (years) | 72 ± 8 | 74 ± 7 | 0.111 |
| Proportion male, $n$ (%) | 15 (83%) | 15 (83%) | — |
| Weight (kg) | 82.7 ± 14.5 | 81.7 ± 14.8 | 0.732 |
| Height (m) | 1.72 ± 0.08 | 1.73 ± 0.10 | 0.866 |
| BMI (kg/m$^2$) | 27.8 ± 4.2 | 27.3 ± 4.1 | 0.665 |
| Whole-body lean mass (kg) | 51.4 ± 9.6 | 50.1 ± 8.3 | 0.492 |
| Whole-body fat mass (kg) | 27.2 ± 6.9 | 27.2 ± 7.7 | 0.990 |
| % body fat | 33.2 ± 5.3 | 33.4 ± 5.2 | 0.651 |
| Clinical characteristics | | | |
| HbA1c (%) | 6.4 ± 0.7 | — | |
| Time since diagnosis (years) | 10 ± 8 | — | |
| Anti-diabetic medications | | | |
| Biguanide | 10 (56%) | — | |
| DPP-4 inhibitor | 7 (39%) | — | |
| SGLT2 inhibitor | 5 (28%) | — | |
| Sulfonylurea | 3 (17%) | — | |
| Insulin | 3 (17%) | — | |
| Incretin mimetic | 1 (6%) | — | |
| None | 6 (33%) | — | |
| Diabetes-related complications | | | |
| Retinopathy | 2 (11%) | — | |
| Nephropathy | 1 (6%) | — | |
| Additional health conditions | | | |
| Hypertension | 10 (56%) | 5 (28%) | |
| Hypercholesterolemia | 10 (56%) | 3 (17%) | |
| Arthritis | 5 (28%) | 4 (22%) | |
| Other[a] | 6 (33%) | 4 (22%) | |
| Meets PA guidelines[b] | 5 (28%) | 9 (50%) | |

BMI, body mass index; DPP-4, dipeptidyl peptidase-4; HbA1c, glycated haemoglobin; HM, healthy matched; PA, physical activity; SGLT2, sodium-glucose transport protein-2; T2D, type 2 diabetes.
Data are mean ± SD or $n$ (%). No statistically significant differences.
[a]Other health conditions include heart disease, gout, benign prostate hyperplasia, and osteoporosis.
[b]Based on the Canadian Society for Exercise Physiology's Physical Activity Guidelines of 150 min per week of moderate-to-vigorous intensity aerobic activity, plus 2 days per week of muscle strengthening activities.

total arm lean mass tended to be 0.5 kg (or 10%) greater in the T2D group compared with the HM group ($P$ = 0.063). Leg and trunk lean mass was similar between groups.

Total leg fat mass was 1.4 kg (or 17%) lower in the T2D group compared with the HM group ($P$ = 0.048, *Table* 2), which may have been driven by the tendency for 14% (0.8 kg) less upper leg fat mass in the T2D group compared with the HM group ($P$ = 0.072). There were no other between-group differences in regional fat mass.

## *Ultrasound measures of muscle and subcutaneous adipose tissue thickness*

Anterior thigh SAT was 0.23 cm thinner in the T2D group compared with the HM group ($P$ = 0.034, *Table* 3). We did not observe any between-group differences in abdominal SAT or muscle thickness.

## *Muscle texture analysis*

Rectus abdominis mean blob size was 0.25 cm$^2$ smaller in the T2D group compared with the HM group ($P$ = 0.045, *Table* 4). We defined blobs as islands of connected hyperechoic pixels, which may represent fat deposits within the muscle.[28] We did not observe any other between-group differences in rectus abdominis texture features.

Rectus femoris mean blob size tended to be 0.03 cm$^2$ smaller in the T2D group compared with the HM group ($P$ = 0.053, *Table* 4). Rectus femoris LBP entropy was 0.06 A. U. (or 1%) greater in the T2D group compared to the HM group ($P$ = 0.007). Images with higher entropy have more randomly scattered pixels, whereas images with lower entropy have more organized pixels, which may imply clearly structured muscle architecture (e.g. television static vs. a checkerboard).[28] We did not observe any other between-group differences in rectus femoris texture features.

## *Physical function, strength, and metabolic subanalysis*

On average, SPPB scores were 1-point lower in the T2D subgroup ($n$ = 14) compared with the HM subgroup ($n$ = 10, *Table* 5). The T2D subgroup also completed more chair stands


DOI: 10.1002/jcsm.12957

**Table 2** DXA regional body composition

| | T2D group ($n$ = 18) | HM group ($n$ = 18) | $P$ value |
|---|---|---|---|
| Lean mass | | | |
| Trunk (kg) | 25.9 ± 5.1 | 25.6 ± 4.1 | 0.806 |
| ALM (kg) | 21.8 ± 4.4 | 20.9 ± 4.0 | 0.239 |
| ALMI (kg/m$^2$) | 7.33 ± 1.18 | 6.97 ± 0.88 | 0.198 |
| Arms (kg) | 5.6 ± 1.4 | 5.1 ± 1.2 | 0.063 |
| Upper arms | 3.3 ± 0.9 | 2.9 ± 0.7 | **0.034** |
| Forearms | 2.3 ± 0.6 | 2.3 ± 0.5 | 0.382 |
| Legs (kg) | 15.5 ± 4.2 | 15.8 ± 3.0 | 0.688 |
| Upper legs | 11.0 ± 2.1 | 10.6 ± 2.0 | 0.410 |
| Lower legs | 5.3 ± 1.0 | 5.2 ± 1.1 | 0.707 |
| Fat mass | | | |
| Trunk (kg) | 15.9 ± 4.7 | 15.0 ± 4.2 | 0.281 |
| Android | 2.7 ± 1.0 | 2.6 ± 0.9 | 0.551 |
| Gynoid | 4.0 ± 1.0 | 4.2 ± 1.2 | 0.206 |
| A/G ratio | 0.67 ± 0.11 | 0.63 ± 0.15 | 0.325 |
| AFM (kg) | 10.1 ± 2.4 | 11.0 ± 4.1 | 0.214 |
| Arms (kg) | 2.9 ± 0.8 | 2.8 ± 1.0 | 0.491 |
| Upper arms | 2.0 ± 0.7 | 1.9 ± 0.8 | 0.544 |
| Forearms | 0.9 ± 0.2 | 0.9 ± 0.2 | 0.479 |
| Legs (kg) | 6.9 ± 2.1 | 8.3 ± 3.2 | **0.048** |
| Upper legs | 5.2 ± 1.2 | 5.9 ± 2.4 | 0.072 |
| Lower legs | 2.1 ± 0.5 | 2.3 ± 0.9 | 0.167 |

A/G ratio, android-to-gynoid ratio; AFM, appendicular fat mass; ALM, appendicular lean mass; ALMI, appendicular lean mass index; HM, healthy matched; T2D, type 2 diabetes.
Significant $P$ values are bolded.

**Table 3** Ultrasound measurements of muscle and SAT thickness

| | T2D group ($n$ = 18) | HM group ($n$ = 18) | $P$ value |
|---|---|---|---|
| Muscle thickness (cm) | | | |
| Abdomen | 0.86 ± 0.22 | 0.87 ± 0.23 | 0.988 |
| Anterior thigh | 2.88 ± 0.82 | 2.64 ± 0.59 | 0.240 |
| SAT thickness (cm) | | | |
| Abdomen | 2.12 ± 0.75 | 2.46 ± 0.79 | 0.094 |
| Anterior thigh | 0.67 ± 0.32 | 0.90 ± 0.58 | **0.034** |

HM, healthy matched; SAT; subcutaneous adipose tissue; T2D, type 2 diabetes.
Data are mean ± SD. Significant $P$ values are bolded.

in 30 s compared with the HM subgroup (three chair stands or ~23%). We did not observe any other significant differences in physical function or Biodex strength outcomes between the subgroups. Fasting serum glucose (+22%), insulin (+104%), and HOMA-IR (+141%) were all significantly greater in the T2D vs. HM subgroup (*Table* 5).

When all participants (T2D and HM) who underwent additional testing were pooled together ($n$ = 24), we observed moderate-to-strong correlations between ultrasound-based muscle measurements and functional outcomes, such as knee extensor strength. For example, maximal knee extensor power during an isokinetic contraction at 60°/s was negatively correlated with rectus femoris mean echointensity ($r$ = −0.416, $P$ = 0.048; *Figure* 3A) and positively correlated with rectus abdominis histogram skew ($r$ = 0.601, $P$ = 0.003; *Figure* 3B). We also observed moderate-to-strong correlations between ultrasound-based muscle measurements and circulating markers of glucose metabolism. For example, HOMA-IR was positively correlated with rectus femoris LBP entropy ($r$ = 0.419, $P$ = 0.042; *Figure* 3C) and rectus abdominis first-order energy ($r$ = 0.441, $P$ = 0.035; *Figure* 3D). All other significant correlations can be found in *Tables* S1–S4.

## Discussion

In this study, we identified regional differences in body composition between older adults with type 2 diabetes or prediabetes vs. non-diabetic participants who were individually matched for age, sex, and % body fat. DXA-derived measurements of upper arm lean mass were greater, and leg fat mass measurements were lower, in the T2D group compared with the HM group. These findings may indicate a novel body composition phenotype specific to older adults with type 2 diabetes or prediabetes, although confirmation of these findings is warranted through larger studies. In addition, we observed between-group differences in ultrasound texture features of the rectus abdominis and rectus femoris muscles. We show, for the first time, that certain muscle texture features were associated with the degree of insulin resistance and muscle strength in older adults, which may point towards ultrasound as a surrogate tool for evaluating metabolic health and physical function, or tracking the progression of type 2 diabetes. In future, approaches leveraging the measurement of the regional body composition differences described herein could aid in the evaluation of metabolic health in older adults.

Despite the lack of differences in appendicular, leg, or trunk lean mass between groups, older adults with type 2 diabetes and prediabetes had greater upper arm lean mass (by DXA) compared with matched controls. Our findings are in contrast to our original hypothesis, which was based on previous studies that reported lower appendicular,[8–11] leg,[11] and trunk[8] lean mass in older adults with type 2 diabetes compared with normoglycaemic controls. Importantly though, these studies did not control for whole-body adiposity, which is directly associated with the distribution of lean mass in both healthy[13] and diabetic[14] adults. In particular, lean mass may be greater in the weight-bearing lower limbs of heavier individuals as a result of regular ambulation with greater body mass. For this reason, we individually matched each older adult with type 2 diabetes or prediabetes to a non-diabetic individual for % body fat (as well as age and sex) in order to tease out differences in the distribution of lean mass related specifically to insulin resistant conditions such as type 2 diabetes and prediabetes. When % body fat was matched there were no between-group differences in DXA-based whole-body lean (or fat) mass. However, the distribution of regional fat and lean mass differed whereby upper arm lean mass was greater, and leg fat mass was lower, in the T2D group compared with the HM group.

**Table 4** Ultrasound-based muscle texture features

| | T2D group ($n$ = 18) | HM group ($n$ = 18) | $P$ value |
|---|---|---|---|
| Rectus abdominis | | | |
| First-order features | | | |
| Mean echointensity | 53 ± 12 | 58 ± 21 | 0.341 |
| Histogram skew | 0.89 ± 0.40 | 0.72 ± 0.25 | 0.243 |
| Histogram kurtosis | 1.13 ± 1.20 | 0.93 ± 0.76 | 0.569 |
| Energy | 0.018 ± 0.004 | 0.019 ± 0.006 | 0.875 |
| Entropy | 4.25 ± 0.22 | 4.19 ± 0.31 | 0.847 |
| Second-order features | | | |
| GLCM energy | 0.023 ± 0.004 | 0.025 ± 0.008 | 0.585 |
| GLCM contrast | 506 ± 329 | 423 ± 380 | 0.768 |
| GLCM correlation | 0.38 ± 0.10 | 0.43 ± 0.16 | 0.651 |
| GLCM homogeneity | 0.075 ± 0.014 | 0.088 ± 0.036 | 0.349 |
| Higher order features | | | |
| LBP energy | 0.028 ± 0.003 | 0.029 ± 0.003 | 0.464 |
| LBP entropy | 4.47 ± 0.15 | 4.50 ± 0.16 | 0.611 |
| Mean blob size ($cm^2$) | 0.07 ± 0.06 | 0.30 ± 0.43 | **0.045** |
| Rectus femoris | | | |
| First-order features | | | |
| Mean echointensity | 46 ± 10 | 49 ± 16 | 0.428 |
| Histogram skew | 1.40 ± 0.26 | 1.33 ± 0.34 | 0.476 |
| Histogram kurtosis | 2.94 ± 1.32 | 2.53 ± 1.52 | 0.380 |
| Energy | 0.017 ± 0.003 | 0.017 ± 0.005 | 0.834 |
| Entropy | 4.28 ± 0.16 | 4.32 ± 0.25 | 0.496 |
| Second-order features | | | |
| GLCM energy | 0.022 ± 0.003 | 0.022 ± 0.006 | 0.913 |
| GLCM contrast | 542 ± 238 | 605 ± 329 | 0.472 |
| GLCM correlation | 0.40 ± 0.11 | 0.42 ± 0.12 | 0.567 |
| GLCM homogeneity | 0.080 ± 0.016 | 0.081 ± 0.024 | 0.954 |
| Higher order features | | | |
| LBP energy | 0.026 ± 0.002 | 0.027 ± 0.003 | 0.523 |
| LBP entropy | 4.65 ± 0.05 | 4.59 ± 0.08 | **0.007** |
| Mean blob size ($cm^2$) | 0.03 ± 0.04 | 0.07 ± 0.08 | 0.053 |

GLCM, grey-level co-occurrence matrix; HM, healthy matched; LBP, local binary pattern; T2D, type 2 diabetes.
Measurements are in arbitrary units, unless indicated otherwise. Data are mean ± SD. Significant $P$ values are bolded.

**Table 5** Physical function, strength, and metabolic subanalysis

| | T2D group ($n$ = 14) | HM group ($n$ = 10) | $P$ value |
|---|---|---|---|
| Physical function and strength | | | |
| SPPB score | 10 ± 2 | 11 ± 1 | **0.033** |
| Gait speed (m/s) | 1.2 ± 0.2 | 1.1 ± 0.2 | 0.653 |
| 6MWT (m) | 508 ± 54 | 518 ± 123 | 0.789 |
| 30-s chair stands (#) | 16 ± 3 | 13 ± 2 | **0.020** |
| Grip strength (kg) | | | |
| Left | 35.3 ± 10.5 | 32.2 ± 8.2 | 0.445 |
| Right | 36.2 ± 9.9 | 35.1 ± 10.1 | 0.790 |
| Isometric peak torque (Nm) | 173 ± 58 | 163 ± 44 | 0.662 |
| Isokinetic 60°/s | | | |
| Peak torque (Nm) | 138 ± 50 | 127 ± 33 | 0.566 |
| Power (W) | 132 ± 45 | 133 ± 35 | 0.924 |
| Isokinetic 180°/s | | | |
| Peak torque (Nm) | 90 ± 39 | 89 ± 25 | 0.948 |
| Power (W) | 244 ± 102 | 280 ± 79 | 0.388 |
| Circulating metabolic markers | | | |
| Glucose (mM) | 6.2 ± 1.1 | 5.1 ± 0.3 | **0.005** |
| Insulin (μIU/mL) | 19.6 ± 13.6 | 9.6 ± 5.1 | **0.038** |
| C-peptide (ng/mL) | 3.2 ± 1.4 | 2.3 ± 0.9 | 0.077 |
| HOMA-IR | 5.3 ± 3.7 | 2.2 ± 1.2 | **0.015** |

6MWT, 6-min walk test; HM, healthy matched; HOMA-IR, homoeostatic model assessment of insulin resistance; SPPB, Short Physical Performance Battery; T2D, type 2 diabetes.
Data are mean ± SD. Significant $P$ values are bolded.


DOI: 10.1002/jcsm.12957

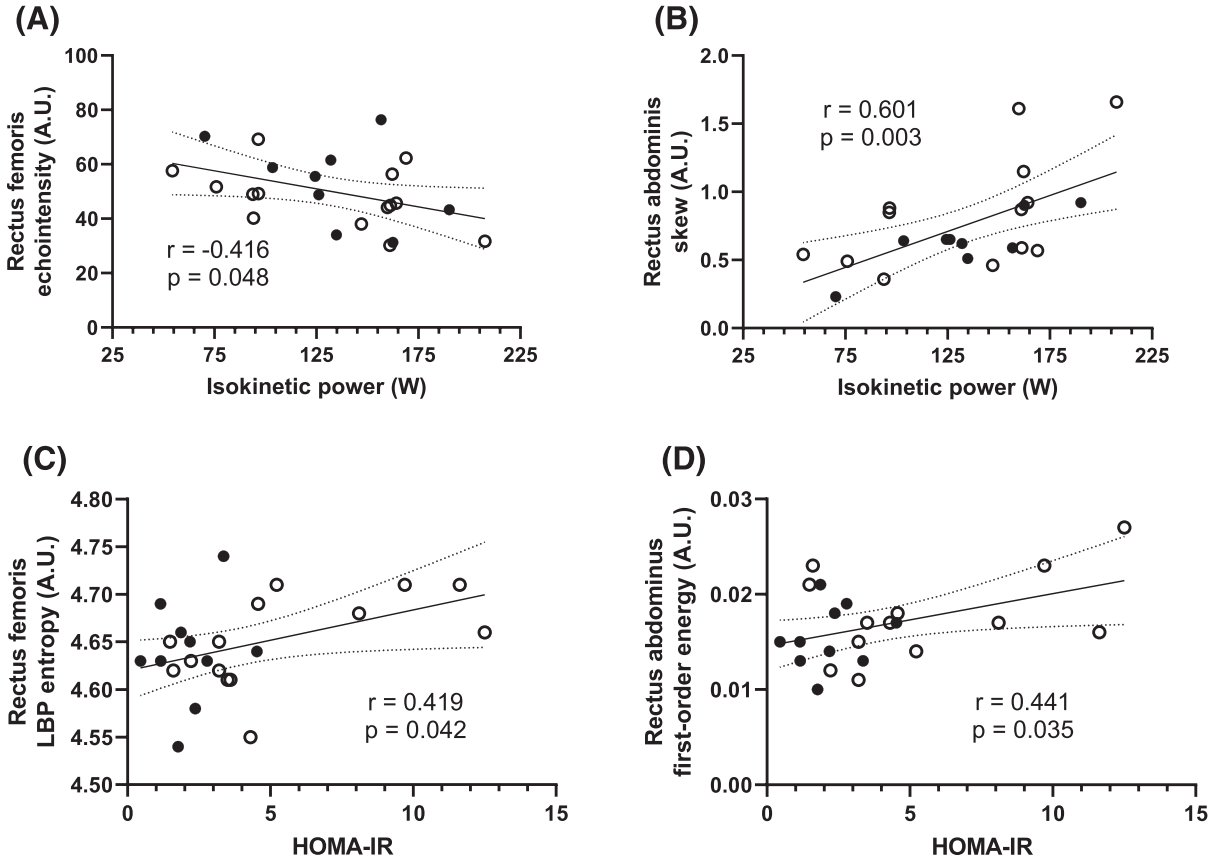


**Figure 3** Ultrasound-based muscle texture features correlate with muscle strength (*A*, *B*) and circulating metabolic markers (*C*, *D*). Two-tailed Pearson correlations were performed on all participants in a single pooled group ($n$ = 24). However, for clarity, the groups are represented by different symbols (T2D group: open circles; HM group: closed circles). HM, healthy matched; HOMA-IR, homoeostatic model assessment of insulin resistance; LBP, local binary pattern; T2D, type 2 diabetes.

Arm lean (and fat) mass is rarely reported in the literature; indeed, leg lean mass, appendicular lean mass index, and trunk fat mass are the regional depots most commonly reported in studies that evaluate body composition in older adult and type 2 diabetic individuals. The emphasis on these depots may be attributed to the well-described loss of appendicular lean mass (leg lean mass, in particular) with age,[29] as well as the association between abdominal obesity and insulin resistance.[30] However, the focus on the lower body and trunk—and the exclusion of the arms—may have prevented previous studies from identifying specific regional body composition changes relevant to this clinical condition. The reason behind our observed difference in upper arm lean mass is unclear but might be related to greater fasting insulin concentrations in the T2D group compared with the matched reference group. Insulin is an anabolic hormone that may protect against muscle atrophy via its inhibitory effect on muscle protein breakdown.[31] In support of this hypothesis, we observed that upper arm lean mass was directly correlated with fasting insulin concentrations. We did not observe a relationship between leg lean mass and circulating insulin, possibly because there was no between-group difference in leg lean mass. But this is speculation that requires further investigation. Future work is needed to confirm if higher upper arm lean mass is a consistent feature of type 2 diabetes and prediabetes and to help better understand the mechanism underpinning it.

Older adults with type 2 diabetes or prediabetes had reduced leg fat mass compared with the matched reference group. We also showed that ultrasound measures of anterior thigh SAT thickness were lower in the T2D group compared to the reference group, suggesting that SAT storage was reduced in older adults with type 2 diabetes or prediabetes. Our findings are supported by Stoney *et al.*[12] and Raška *et al.*,[6] who observed lower leg fat mass in older females with type 2 diabetes compared with BMI-matched and weight-matched controls, respectively. Leg fat, and thigh SAT in particular, may be protective against metabolic disease,[32] possibly due to inherent differences in tissue quality between SAT and ectopic fat, such as intermuscular and visceral adipose tissue. Adipocytes isolated from leg fat have been shown to secrete more adiponectin (an adipokine positively associated with insulin sensitivity)[33] and take up greater quantities of circulating non-esterified fatty acids,[34]

compared with adipocytes isolated from the abdominal region. Therefore, our observations of reduced thigh SAT and leg fat in older adults with type 2 diabetes or prediabetes is consistent with the metabolic impairments that characterize this population. Our findings also emphasize the importance of using tools like ultrasound, which (in contrast to DXA) allow for the measurement of SAT as well as muscle.

Echointensity is a commonly reported first-order ultrasound texture feature that may be indicative of tissue quality. [35] However, given that echointensity comprises the average brightness of all pixels, it may not be sensitive enough to capture important features in tissue quality within the imaged region. Second-order and high-order texture analysis, which incorporates the spatial arrangement of two or more pixels, can identify patterns in the ultrasound image and, as such, may provide a more robust indication of tissue quality. Indeed, in the present study, although we did not observe between-group differences in mean echointensity, older adults with type 2 diabetes or prediabetes exhibited distinct ultrasound-based higher order muscle texture features compared to matched normoglycaemic controls. Specifically, rectus femoris LBP entropy was higher, and rectus abdominis mean blob size was smaller, in the T2D group. Considering that both abdominal and anterior thigh muscle thicknesses were similar between groups, these texture differences likely represent differences in tissue quality and composition. Because LBP entropy is a measurement of pixel randomness, our observations may indicate rectus femoris deterioration or reduced tissue organization in the type 2 diabetes/prediabetes group. Reduced rectus abdominis blob size, on the other hand, may represent smaller fatty deposits. However, further work is needed to determine the physiological meaning of these texture features.

Higher order texture features of muscle ultrasound images reflect pixel organization and have previously been used to assess muscle damage and track disease progression in myopathies such as amyotrophic lateral sclerosis.[36] As well, higher order texture features are distinct in males vs. females,[26] older vs. younger adults,[37] and across individual muscles (e.g. biceps brachii vs. biceps femoris vs. tibialis anterior).[26] Previous work using muscle biopsies[38] and magnetic resonance imaging[16] has also shown that ultrasound-based texture features correspond to both intramuscular and intermuscular adipose tissue, respectively. Given that higher quantities of intramuscular and intermuscular adipose tissue are positively associated with insulin resistance, and negatively associated with quadriceps strength, we hypothesized that ultrasound-based texture features would reflect metabolic health and physical function in our group of participants. We are the first to report that multiple texture features of two distinct muscles (rectus femoris and rectus abdominis) were significantly correlated with HOMA-IR and muscle power (during an isokinetic contraction) in a subgroup of older adults in this study. Because we did not observe any significant between-group difference in muscle strength, our study suggests that ultrasound texture features may represent a novel and non-invasive method of tracking metabolic health and physical function in older adults. Future studies are needed to confirm our findings, as well as to determine whether texture features of other muscle groups are associated with insulin resistance.

There are several limitations to the present study. Although we recruited a relatively small and heterogeneous group of patients, each patient was tightly and individually matched to a non-diabetic control for age, sex, and % body fat to augment our ability to detect between-group differences. We included any older adult with type 2 diabetes or prediabetes, regardless of sex or treatment regimen. Given the influence of sex and insulin therapy on weight and body composition, this may have increased the variability of our measurements. Some hypoglycaemic medications, such as biguanides and sulfonylureas, have been shown to promote muscle atrophy, while others, such as SGLT-2 inhibitors, are associated with lean mass preservation.[39] Importantly, most patients in the current study were taking more than one anti-diabetic drug, and the effect of multiple anti-diabetic drugs on body composition is not well-understood. Lastly, we did not assess nutrition or an objective measurement of physical fitness, which may have helped to explain differences in fat and lean mass between older adults with type 2 diabetes and matched controls.

In conclusion, we present evidence for a unique body composition phenotype specific to older adults with type 2 diabetes and prediabetes, which was characterized by greater lean mass in the upper arm and reduced leg fat mass compared with a matched normoglycaemic reference group. We also showed, for the first time, that (i) ultrasound-based muscle texture features differ between older adults with type 2 diabetes or prediabetes and non-diabetics, and (ii) certain thigh and abdominal muscle texture features align with the degree of insulin resistance and physical function. Altogether, this study provides evidence for new phenotypic and ultrasound markers of metabolic health and physical function in older adults. Further work is warranted to confirm our findings and to uncover the mechanisms underpinning these distinct regional distributions of lean and fat mass in older adults with type 2 diabetes or prediabetes.

## Acknowledgements

We thank Janice Skafel, Stephanie Auer, and Alicia Nadon for coordinating and performing the DXA scans for this study. The authors of this manuscript certify that they comply with the ethical guidelines for authorship and publishing in the Journal of Cachexia, Sarcopenia and Muscle.[40] This study received clearance from the University of Waterloo Office of

Research Ethics and was performed in accordance with the 1964 Declaration of Helsinki and its later amendments. All participants provided written informed consent prior to taking part in the study.

## Online supplementary material

Additional supporting information may be found online in the Supporting Information section at the end of the article.

## Funding

This study was funded by a Canada Foundation for Innovation grant (to MM). KEB was supported by a Canadian Institutes of Health Research (CIHR) Fellowship, and MTP was supported by a CIHR Doctoral Award.

## Conflicts of interest

KEB, MTP, EA, and MM declare that they have no conflict of interest.

## References

1. DeFronzo RA. Glucose intolerance and aging. *Diabetes Care* 1981;**4**:493–501.
2. Zamboni M, Zoico E, Scartezzini T, Mazzali G, Tosoni P, Zivelonghi A, et al. Body composition changes in stable-weight elderly subjects: the effect of sex. *Aging Clin Exp Res* 2003;**15**:321–327.
3. Kuk JL, Saunders TJ, Davidson LE, Ross R. Age-related changes in total and regional fat distribution. *Ageing Res Rev* 2009;**8**: 339–348.
4. Nordstrom A, Hadrevi J, Olsson T, Franks PW, Nordstrom P. Higher prevalence of type 2 diabetes in men than in women is associated with differences in visceral fat mass. *J Clin Endocrinol Metab* 2016; **101**:3740–3746.
5. Wang T, Feng X, Zhou J, Gong H, Xia S, Wei Q, et al. Type 2 diabetes mellitus is associated with increased risks of sarcopenia and pre-sarcopenia in Chinese elderly. *Sci Rep* 2016;**6**:38937.
6. Raška I Jr, Raškova M, Zikán V, Škrha J. Body composition is associated with bone and glucose metabolism in postmenopausal women with type 2 diabetes mellitus. *Physiol Rev* 2017;**66**:99–111.
7. Yoon JW, Ha YC, Kim KM, Moon JH, Choi SH, Lim S, et al. Hyperglycemia is associated with impaired muscle quality in older men with diabetes: the Korean Longitudinal Study on Health and Aging. *Diabetes Metab J* 2016;**40**:140–146.
8. Park SW, Goodpaster BH, Lee JS, Kuller LH, Boudreau R, de Rekeneire N, et al. Excessive loss of skeletal muscle mass in older adults with type 2 diabetes. *Diabetes Care* 2009;**32**:1993–1997.
9. Kim TN, Park MS, Yang SJ, Yoo HJ, Kang HJ, Song W, et al. Prevalence and determinant factors of sarcopenia in patients with type 2 diabetes: the Korean Sarcopenic Obesity Study (KSOS). *Diabetes Care* 2010;**33**: 1497–1499.
10. Kim KS, Park KS, Kim MJ, Kim SK, Cho YW, Park SW. Type 2 diabetes is associated with low muscle mass in older adults. *Geriatr Gerontol Int* 2014;**14**:115–121.
11. Leenders M, Verdijk LB, van der Hoeven L, Adam JJ, van Kranenburg J, Nilwik R, et al. Patients with type 2 diabetes show a greater decline in muscle mass, muscle strength, and functional capacity with aging. *J Am Med Dir Assoc* 2013;**14**: 585–592.
12. Stoney RM, Walker KZ, Best JD, Ireland PD, Giles GG, O'Dea K. Do postmenopausal women with NIDDM have a reduced capacity to deposit and conserve lower-body fat? *Diabetes Care* 1998;**21**: 828–830.
13. Forbes GB. Lean body mass-body fat interrelationships in humans. *Nutr Rev* 1987;**45**: 225–231.
14. Fukuoka Y, Narita T, Fujita H, Morii T, Sato T, Sassa MH, et al. Importance of physical evaluation using skeletal muscle mass index and body fat percentage to prevent sarcopenia in elderly Japanese diabetes patients. *J Diabetes Investig* 2019;**10**: 322–330.
15. Forbes GB, Welle SL. Lean body mass in obesity. *Int J Obes (Lond)* 1983;**7**:99–107.
16. Young H-J, Jenkins NT, Zhao Q, McCully KK. Measurement of intramuscular fat by muscle echo intensity. *Muscle Nerve* 2015;**52**: 963–971.
17. Jacob S, Machann J, Rett K, Brechtel K, Volk A, Renn W, et al. Association of increased intramyocellular lipid content with insulin resistance in lean nondiabetic offspring of type 2 diabetic subjects. *Diabetes* 1999; **48**:1113–1119.
18. Park H-S, Lim JS, Lim S-K. Determinants of bone mass and insulin resistance in Korean postmenopausal women: muscle area, strength, or composition? *Yonsei Med J* 2019;**60**:742–750.
19. Akazawa N, Kishi M, Hino T, Tsuji R, Tamura K, Moriyama H. Increased intramuscular adipose tissue of the quadriceps is more strongly related to declines in ADL than is loss of muscle mass in older inpatients. *Clin Nutr* 2021;**40**:1381–1387.
20. Paris MT, Bell KE, Avrutin E, Mourtzakis M. Ultrasound image resolution influences analysis of skeletal muscle composition. *Clin Physiol Funct Imaging* 2020;**40**: 277–283.
21. Paris MT, Lafleur B, Dubin JA, Mourtzakis M. Development of a bedside viable ultrasound protocol to quantify appendicular lean tissue mass. *J Cachexia Sarcopenia Muscle* 2017;**8**:713–726.
22. Nana A, Slater GJ, Hopkins WG, Burke LM. Techniques for undertaking dual-energy X-ray absorptiometry whole-body scans to estimate body composition in tall and/or broad subjects. *Int J Sport Nutr Exerc Metab* 2012;**22**: 313–322.
23. Baumgartner R, Koehler K, Gallagher D, Romero L, Heymsfield SB, Ross RR, et al. Epidemiology of sarcopenia among the elderly in New Mexico. *Am J Epidemiol* 1998;**147**:755–763.
24. Castellano G, Bonilha L, Li LM, Cendes F. Texture analysis of medical images. *Clin Radiol* 2004;**59**:1061–1069.
25. Hall-Beyer M. Practical guidelines for choosing GLCM textures to use in landscape classification tasks over a range of moderate spatial scales. *Int J Remote Sensing* 2017;**38**:1312–1338.
26. Molinari F, Caresio C, Acharya UR, Mookiah MR, Minetto MA. Advances in quantitative muscle ultrasonography using texture analysis of ultrasound images. *Ultrasound Med Biol* 2015;**41**:2520–2532.
27. Nielsen PK, Jensen BR, Darvann T, Jørgensen K, Bakke M. Quantitative ultrasound tissue characterization in shoulder and thigh muscles—a new approach. *BMC Musculoskelet Disord* 2006;**7**:https://doi.org/10.1186/1471-2474-7-2
28. Paris MT, Mourtzakis M. Muscle composition analysis of ultrasound images: a narrative review of texture analysis. *Ultrasound Med Biol* 2021;**47**:880–895.
29. Abe T, Sakamaki M, Yasuda T, Bemben MG, Kondo M, Kawakami Y, et al. Age-related, site-specific msucle loss in 1507 Japanese men and women aged 20-95 years. *J Sports Sci Med* 2011;**10**:145–150.

30. Tchernof A, Després J-P. Pathophysiology of human visceral obesity: an update. *Physiol Rev* 2013;**93**:359–404.
31. Nygren J, Nair KS. Differential regulation of protein dynamics in splanchnic and skeletal muscle beds by insulin and amino acids in healthy human subjects. *Diabetes* 2003; **52**:1377–1385.
32. Zhang X, Hu EA, Wu H, Malik V, Sun Q. Associations of leg fat accumulation with adiposity-related biological factors and risk of metabolic syndrome. *Obesity* 2013;**21**: 824–830.
33. Fain JN, Madan AK, Hiler ML, Cheema P, Bahouth SW. Comparison of the release of adipokines by adipose tissue, adipose tissue matrix, and adipocytes from visceral and subcutaneous abdominal adipose tissues of obese humans. *Endocrinology* 2004;**145**:2273–2282.
34. Shadid S, Koutsari C, Jensen MD. Direct free fatty acid uptake into human adipocytes in vivo: relation to body fat distribution. *Diabetes* 2007;**56**:1369–1375.
35. Mourtzakis M, Parry S, Connolly B, Puthucheary Z. Skeletal muscle ultrasound in critical care: a tool in need of translation. *Ann Am Thorac Soc* 2017;**14**: 1495–1503.
36. Martínez-Payá JJ, Ríos-Díaz J, Medina-Mirapeix F, Vázquez-Costa JF, del Baño-Aledo ME. Monitoring progression of amyotrophic lateral sclerosis using ultrasound morpho-textural muscle biomarkers: a pilot study. *Ultrasound Med Biol* 2018;**44**: 102–109.
37. Watanabe T, Murakami H, Fukuoka D, Terabayashi N, Shin S, Yabumoto T, et al. Quantitative sonographic assessment of the quadriceps femoris muscle in healthy Japanese adults. *J Ultrasound Med* 2017; **36**:1383–1395.
38. Reimers K, Reimers C, Wagner S, Paetzke I, Pongratz DE. Skeletal muscle sonography: a correlative study of echogenicity and morphology. *J Ultrasound Med* 1993; **2**:73–77.
39. Inoue H, Morino K, Ugi S, Tanaka-Mizuno S, Fuse K, Miyazawa I, et al. Ipragliflozin, a sodium-glucose cotransporter 2 inhibitor, reduces bodyweight and fat mass, but not muscle mass, in Japanese type 2 diabetes patients treated with insulin: a randomized clinical trial. *J Diabetes Investig* 2019;**10**: 1012–1021.
40. von Haehling S, Morley JE, Coats AJS, Anker SD. Ethical guidelines for publishing in the journal of cachexia, sarcopenia and muscle: update 2021. *J Cachexia Sarcopenia Muscle* 2021;**12**:2259–2261.